Reproduced from Soil Science Society of America Journal. Published by Soil Science Society of America. All copyrights reserved.

The Dielectric Permittivity of Calcite and Arid Zone Soils with Carbonate Minerals

I. Lebron,* D. A. Robinson, S. Goldberg, and S. M. Lesch

ABSTRACT

Measurement of soil dielectric properties, ε are widely used to estimate water content in soils from remote sensing and from in situ soil sensors such as time domain reflectometry (TDR). The mineral permittivity also plays an important role in geochemical dissolution and precipitation. Models used to estimate water content from soils often assume a value of 5 for the mineral permittivity ε_s. However, calcite ($CaCO_3$), a major constituent of some arid and semi-arid soils, has a permittivity of 8 to 9, nearly twice the permittivity of quartz ($\varepsilon_s = 4.6$). We studied four soils, with micaceous mineralogy, but with two soils having approximately 40% calcite. We also measured the permittivity of Iceland Spar calcite ($\varepsilon_s = 9.1$) and a microcrystalline calcite ($\varepsilon_s = 8.3$), and use atomistic modeling to account for differences in permittivity based on the crystal density. We found permittivities for our soils to be in the range of 5.8 to 6.6, higher calcite contents resulting in increased permittivity. The estimated permittivity of the calcite in the soils was 7.4 to 7.9, lower than the highly crystalline samples. We estimate, for a soil with a porosity of 0.5 that assuming a permittivity of 5 instead of 6.6 will result in an overestimation of water content of about 1% at saturation. This demonstrates that a large quantity of pedogenic calcite (40%) in soil is unlikely to cause substantial error in the determination of water content using standard calibration equations. However, the lower dielectric permittivity predicted for pedogenic calcite may have consequences for the interpretation and understanding of geochemical processes.

The development of electromagnetic sensor technology toward the end of the last century increased interest in the measurement of soil properties using electromagnetic techniques. The determination of soil water content from the measurement of soil dielectric permittivity has become a widely accepted method (Topp et al., 1980; Topp and Ferre, 2002; Robinson et al., 2003). Investigations have also explored the use of dielectric measurement to estimate other soil properties such as cation exchange capacity (Fernando et al., 1977), soil aggregation (Miyamoto et al., 2003), and particle-size analysis (Starr et al., 2000). Understanding the dielectric properties of soils is also required for the improved interpretation of data from methods such as ground penetrating radar (Huisman et al., 2001; Davis and Annan, 2002) and microwave remote sensing (McNairn et al., 2002). Modeling of the dielectric properties of granular materials such as soils cannot only improve calibration models and techniques to monitor properties, but also lead to new methods of material characterization. When modeling a composite material such as soil it is required that the dielectric permittivity of all phases (solid, liquid, and gas) are known, especially if the model is to be used to predict water content or porosity. The permittivity of air and water are well documented (Lide, 1999). However, a value of 5 reflecting the permittivity of quartz (4.19 to 5.00; Keller, 1989) is often used as an input parameter for the permittivity of the solid for modeling (Friedman, 1998).

I. Lebron, S. Goldberg, and S.M. Lesch, USDA-ARS, George E. Brown, Jr. Salinity Lab., 450 W. Big Springs Rd, Riverside, CA 92507; D.A. Robinson and currently I. Lebron, Dep. of Plants, Soils and Biometerology, Utah State Univ., Logan, UT 84322. Received 3 Oct. 2003. *Corresponding author (inma_lebron@yahoo.com).

Published in Soil Sci. Soc. Am. J. 68:1549–1559 (2004).
© Soil Science Society of America
677 S. Segoe Rd., Madison, WI 53711 USA

Geochemical Importance of the Mineral Permittivity

Water is an excellent solvent, primarily because of its high dielectric constant, approximately 80. For a continuum scale analysis, the inverse square Coulomb force between two charged atoms is reduced by a factor determined by the permittivity of the medium surrounding them. The free energy, $w(r)$ of the Coulomb interaction between two charges Q_1 and Q_2 is:

$$w(r) = \frac{Q_1 Q_2}{4\pi\varepsilon_o\varepsilon_e r} \quad [1]$$

where ε_e is the permittivity of the surrounding or environment, ε_o is the permittivity of free space (8.854 pF m^{-1}) and r is the distance between the two charges. This indicates the importance of the permittivity of the environment in determining how the charges feel each other. A step further takes us to the *Born* or *solvation* energy of an ion (μ^i). The Born energy, a positive quantity, gives the electrostatic free energy of an ion in a medium of permittivity ε_e:

$$\mu_i = \frac{Q^2}{8\pi\varepsilon_o\varepsilon_e a} \quad [2]$$

where Q is the charge of the ion and, a is the radius of the ion. This can now be used to calculate the change in free energy ($\Delta\mu^i$, joules) of moving an ion from a medium of low dielectric constant, ε_e to a medium of high dielectric constant ε_b.

$$\Delta\mu^i = -\frac{Q^2}{8\pi\varepsilon_o a}\left[\frac{1}{\varepsilon_e} - \frac{1}{\varepsilon_b}\right] \quad [3]$$

The transfer of the ion from ε_e to ε_b results in negative values and thus it is energetically favorable. For a full derivation of the above equations see Israelachvili (1992). This is the core to explaining why ionic solids dissolve in polar liquids. Molecular models describing calcite, as represented by Fisler et al. (2000), represent predominantly ionic bonding and include refinements for covalency and electronic polarization. These atomistic models of carbonate minerals still use a modified form of the Born model to describe atomic interaction within the crystal (Fisler et al., 2000; Cygan et al., 2002). Thus the contrast between the permittivity of the calcite

Abbreviations: TDR, time domain reflectometry.

Reproduced from Soil Science Society of America Journal. Published by Soil Science Society of America. All copyrights reserved.

crystal and the bathing solution may have a role in determining mineral solubility.

Many arid soils contain large quantities of salts, while the more soluble ones are prone to dissolving and being transported, more insoluble salts like calcite precipitate. Over time this can amount to large quantities when the water has excess in Ca and bicarbonates. Calcite in soils does not precipitate by crystal growth but by heterogeneous nucleation (Lebron and Suarez, 1996). That is the reason why in soils, well-developed pedogenic crystals of calcite are not encountered. The presence of water-soluble organic ligands and ions such as PO_4^{-3} act as precipitation inhibitors by blocking crystal growth sites (Paquette et al., 1995; Lebron and Suarez, 1996, 1998). The presence of other cations like Mn, common in soil environments, may cause coprecipitation or formation of solid solutions with the result of mixed crystals of variable chemical composition (Lebron and Suarez, 1999). Consequently, it is expected that the dielectric permittivity of pedogenic calcite will differ from the permittivity of perfectly crystalline calcite. Crystals formed by crystal growth in the absence of impurities and without isomorphic substitutions provide pristine crystals where the ions are translationally symmetric and ordered without imperfections or abrupt interruptions. Tabulated permittivity values for calcite generally refer to pure crystalline samples.

Measurement of Solid Phase Permittivity

Permittivity values for other commonly occurring soil minerals are difficult to find and are often estimated using two-phase mixing models rather than measured. Olhoeft (1979) pioneered much of the estimation of rock mineral permittivity using two-phase mixing models to provide tables of estimated mineral permittivity values (Olhoeft, 1981; Carmichael, 1982; Nelson et al., 1989; Nelson and You, 1990; Nelson, 1992). These tabulated values are very useful in indicating that the permittivity of some minerals is much greater than others. However, the method is unreliable in terms of obtaining absolute values. It relies on applying a two-phase (air and solid) dielectric mixing model to calculate the permittivity of a granular sample repacked in air, with the permittivity extrapolated to zero porosity. This method pre-assumes the correctness of the mixing model. Soils prove difficult materials for accurately estimating their solid permittivity. Predicted permittivity values for the same mineral can vary considerably depending on the choice of mixing model. Particle shapes and sizes and the presence of clay minerals that may be partially hydrated can influence the accuracy of the estimates. An additional complexity in soil systems is the variable chemical composition of minerals. Isomorphic substitutions and solid solutions are intrinsic to pedogenic conditions. Consequently, the chemical formula for clays and minerals are not unique.

In recent work, Robinson and Friedman (2003) presented a method, using a TDR probe, to measure the solid dielectric permittivity of granular materials. This method measures the effective permittivity of granular samples when immersed in different dielectric liquids. The liquids are chosen to obtain values of effective permittivity lower and higher than the expected solid permittivity. The permittivity value for the solid is obtained when the fluid permittivity matches the effective permittivity of the mixture or by interpolation to that point. The method is very effective and produces permittivity values for granular quartz in close agreement with measurements presented in the literature for single crystals. Recently the method was refined for clay minerals and fine-grained materials (Robinson, 2004a).

Our objectives for this work are: (i) to quantify the contribution of pedogenic calcite to the solid dielectric permittivity of soils with calcite, and draw implications for estimating water content, and (ii) to compare the permittivity of the pedogenic calcite with pristine calcite specimens of different origin, and draw implications for soil geochemical processes.

THEORY

Two-Phase Single Solid Dielectric in Dielectric Solution

The immersion of a granular material in a dielectric fluid gives an effective permittivity, ε_{eff} somewhere between the permittivity of the background ε_e, and the permittivity of the granular inclusions ε_s. The Maxwell-Garnett (1904) mixing model based on the Lord Rayleigh (1892) formula is commonly used for describing a two-phase mixture (Sihvola, 1999) and best suited to the present discussion:

$$\varepsilon_{eff} = \varepsilon_e + 3f\varepsilon_e\left[\frac{\varepsilon_s - \varepsilon_e}{\varepsilon_s + 2\varepsilon_e - f(\varepsilon_s - \varepsilon_e)}\right] \qquad [4]$$

where, f is the fraction of the solid, $f = (1 - \phi)$, ϕ is porosity. The model does not account for the effects of particle close packing but this is minimal when the contrast ($\varepsilon_e/\varepsilon_s$) between the two phases is <3 (Robinson and Friedman, 2002). The model assumes that the solid spherical inclusions 'see' only the permittivity of the background. In practice in a densely packed granular material the background seen by the solid is some combination of solid and fluid and its respective permittivity. The Maxwell-Garnett model provides an upper bound where the background has a higher permittivity than the inclusion and a lower bound when this is reversed.

Figure 1 shows the relationship between the effective permittivity, ε_{eff}, and the fluid permittivity, ε_e, for a granular sample with $\varepsilon_s = 5$, packed to three different porosities. The 1:1 line is plotted on the diagram and it can be seen that all the lines converge at the value of 5 when the solid and fluid have the same permittivity. Below this point the effective permittivity of the mixture is higher than the solution and above this point the effective permittivity is lower than the permittivity of the immersion fluid. The main point demonstrated by the modeling is that for a fixed porosity the effective permittivity and the solution permittivity have the same value at a unique point equivalent to the permittivity of the solid.

Two-Phase Binary Solid Dielectrics in Dielectric Solution

Another aspect to consider when dealing with soils is how to account for the effective permittivity of a material with inclusions of different volume fractions and different permittivities. Sihvola (1999) presented a simple Maxwell-Garnett

Reproduced from Soil Science Society of America Journal. Published by Soil Science Society of America. All copyrights reserved.

based model for spherical inclusions for this problem. He demonstrated that the permittivity of the solid was not simply the arithmetic average of the solid permittivities and their respective volume fractions:

$$\varepsilon_{eff} = \varepsilon_e + 3\varepsilon_e \frac{\left[f_1\left(\frac{\varepsilon_1 - \varepsilon_e}{\varepsilon_1 + 2\varepsilon_e}\right) + f_2\left(\frac{\varepsilon_2 - \varepsilon_e}{\varepsilon_2 + 2\varepsilon_e}\right)\right]}{1 - \left[f_1\left(\frac{\varepsilon_1 - \varepsilon_e}{\varepsilon_1 + 2\varepsilon_e}\right) + f_2\left(\frac{\varepsilon_2 - \varepsilon_e}{\varepsilon_2 + 2\varepsilon_e}\right)\right]} \quad [5]$$

where, f_1 is the fraction of solid with permittivity ε_1 and f_2 is the volume fraction of solid with a permittivity ε_2. Robinson and Friedman (2002) presented work on the dielectric properties of mixtures of glass beads and quartz sand. They demonstrated that in the case of low contrasts ($\varepsilon_2/\varepsilon_1 < 3$) between the inclusion permittivity values, as is the case with soil minerals, negligible error was obtained by referring to a single ε_s, which is the arithmetic average of the permittivity of the minerals and their volume fractions.

MATERIALS AND METHODS

Soils

Four micaceous/illitic soils were chosen for this study: Ramona and Clarence, from the USA, and two soils from the Ebro Basin (Spain). Classification and dominant mineralogy are shown in Table 1, particle-size distribution, Fe and Al oxide, organic matter, and calcite content are shown in Table 2. Granulometric determinations were made in a Sedigraph 5000ET (Micromeritics, Norcross, GA[1]), Fe and Al oxides were extracted by the method of Jackson et al. (1986). Inorganic and organic C was analyzed by a CO_2 coulometer (UIC Corp., Joliet, IL). Mineralogical identification was performed by x-ray powder diffraction. We removed the calcite from a portion of the two soils from the Ebro Basin according to the method described in Kunze and Dixon (1986). Mineralogical identification was performed by x-ray powder diffraction to ensure total calcite removal (Fig. 2).

Calcite Minerals

The properties of the calcite minerals used in this study are shown in Table 3. Particle densities were determined using the excluded volume method described in Flint and Flint (2002). The calcite powder was obtained from Pfizer (Multiflex MM from Pfizer, Los Angeles, CA), the Iceland Spar was from Ward's (Ward's Natural Science Establishment Inc., New York). Characterization of the morphology, size, and crystallinity was done using microscopic and x-ray techniques. Figure 3a shows a micrograph of the Iceland Spar using a scanning electron microscope (AMRAY, 3200, AMRAY Inc., Bedford, MA). Crystallinity was analyzed by selected area electron diffraction for Iceland Spar (Fig. 3b) (SAED, Philips Analytical, Eindhoven, the Netherlands). Figure 3c shows the micrograph of the microcrystalline calcite using a transmission electron microscope, and the x-ray diffraction pattern using energy dispersive X-ray (EDX) (Fig. 3d) (Philips CM 300, Philips Analyitical, Eindhoven, the Netherlands).

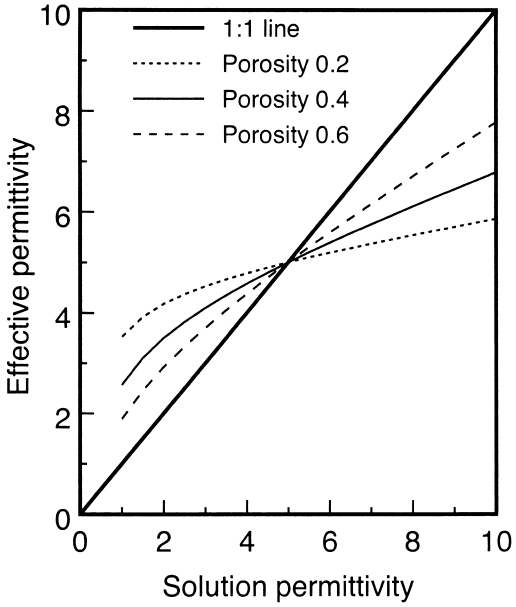

Fig. 1. Modeled effective permittivity (Eq. [1]) of a two-phase mixture plotted vs. the permittivity of the background solution at different porosities. The unique crossing point occurs when the permittivity of the fluid matches the permittivity of the solid.

Dielectric Immersion Fluids

We used the method described in Robinson (2004a) to measure the dielectric permittivity of fine-grained granular materials. The critical aspect in applying this method is finding fluids whose permittivities lie in a range between 1 and 15 to provide the dielectric background. Furthermore, the characteristics of the background fluids are important, they must not exhibit strong relaxation at the frequency of measurement (0.1–1 GHz). Robinson and Friedman (2003) used air, $\varepsilon = 1$; penetrating oil (WD-40, WD-40 Company, San Diego, CA), $\varepsilon = 2.3$; methylene chloride, $\varepsilon = 8.8$; and acetone, $\varepsilon = 20.8$. They also found that the alcohols were unsuitable because of relaxation in the frequency bandwidth of the TDR. In this work mixtures of fluids were used to obtain the low permittivity background dielectric solutions. The main fluids used were: air, $\varepsilon = 1$; corn oil, $\varepsilon = 2.4'$ dicholoromethane, $\varepsilon = 9.1$; and acetone, $\varepsilon = 20.8$, at 25°C. The acetone and corn oil are miscible, which allowed us to prepare dielectric background solutions with a permittivity between 2.4 and 20.8.

Measurement of the Effective Permittivity and TDR Probe Construction

A Tektronix (1502C) TDR cable tester and a custom made coaxial TDR probe were used throughout the experiments to measure the effective permittivity of soil and clay suspensions. The TDR was connected to a personal computer, which was used to collect and analyze waveforms using software developed by Heimovaara and de Water (1993). Cable tester and

[1]Trade names are provided for the benefit of the reader and do not imply any endorsement by the USDA.

Table 1. Classification and dominant mineralogy of the four soils studied, Ramona and Clarence soils according to U.S. Taxonomy.

Soil	Origin	Classification	Mineralogy
Ramona	California	fine-loamy, mixed, thermic Typic Haploxeralf	Mica di- and trioctahedral
Clarence	Illinois	fine, illitic, mesic Aquic Argiuoll	Mica dioctahedral
Ebro Basin soils EB1 and EB2	Spain	fine, illitic, xeric, alkaline	Mica dioctahedral

Reproduced from Soil Science Society of America Journal. Published by Soil Science Society of America. All copyrights reserved.

Table 2. Particle-size distribution and other components of the soils in this study.

	Clay (<2 μm)	Silt (2–50 μm)	Sand (>50 μm)	Fe_2O_3	Al_2O_3	Organic C	$CaCO_3$
	%						
Ramona	8.8	21.4	69.8	0.49	0.70	0.87	none
Clarence	79.6	18.7	1.7	1.38	0.25	0.34	none
Ebro Basin 1	25.7	69.2	5.1	1.94	0.38	0.13	41
Ebro Basin 2	30.8	64.7	4.4	2.06	0.43	0.39	35

probe were connected via a 0.75 m, (50-ohm RG 58) coaxial cable. The probe had an internal stainless steel electrode (A in Fig. 4), 0.003175 m in diameter and 0.16 m in total length with 0.152 m projecting above the chemical resistant delrin probe head (Dupont, Wilmington, DE). The outer part of the TDR probe was a brass cylinder (B in Fig. 4) 0.156 m long with an internal diameter of 0.085 m. This cylinder had a brass collar soldered onto it at one end so that a screw fitting (C in Fig. 4) could tighten the coaxial cell onto the microwave electrical connector (E in Fig. 4). The central electrode had a male shaped end that fitted into the female microwave connector (E in Fig. 4). The microwave electrical connector was high quality and rated to pass frequencies of up to 11 GHz. The coaxial TDR probe was designed with a screw and push fit to allow separation and cleaning. A small probe was developed to minimize the amount of clay mineral required for the measurement. The volume of the cell was 8.0134 cm^3. The TDR probe was calibrated for effective length (0.154 m) using air and deionized water (Heimovaara, 1993; Robinson et al., 2003).

Measurement Procedure

The measurement procedure relies on making a suspension of the mineral in the background dielectric fluid. In the first step, soils and mineral samples were oven dried at 150°C overnight to remove any hygroscopic water. The samples were removed from the oven and allowed to cool in a desiccator. A 10-g subsample from the dessicator was removed and accurately weighed in a plastic weighing boat on a four-point balance. The sample was then gently poured into the coaxial TDR probe until it was flush with the top, thus forming a loose packing, measurements were then made. The weighing boat was then reweighed with the remaining material to determine the mass of sample poured into the probe. The solid was then removed from the coaxial probe and the probe was dismantled and cleaned.

The second set of measurements was then made, initially by measuring the permittivity of the liquid. The solid–liquid suspension was then made by removing the fluid from the probe using a large syringe with a 0.16-m tube attached. The suspension was made using this fluid, maintained at the same temperature in a 10-mL syringe (Fig. 4, G). The nozzle of the syringe was blocked with a stopper and 4 mL of liquid was placed in the 10-mL syringe. The weighed mineral sample was poured into the syringe and mixed using a stainless steel stirring rod (Fig. 4, H). The suspension sample was now made up to a mark on the syringe representing 8.0 cm^3. The stopper was removed from the nozzle and another syringe attached

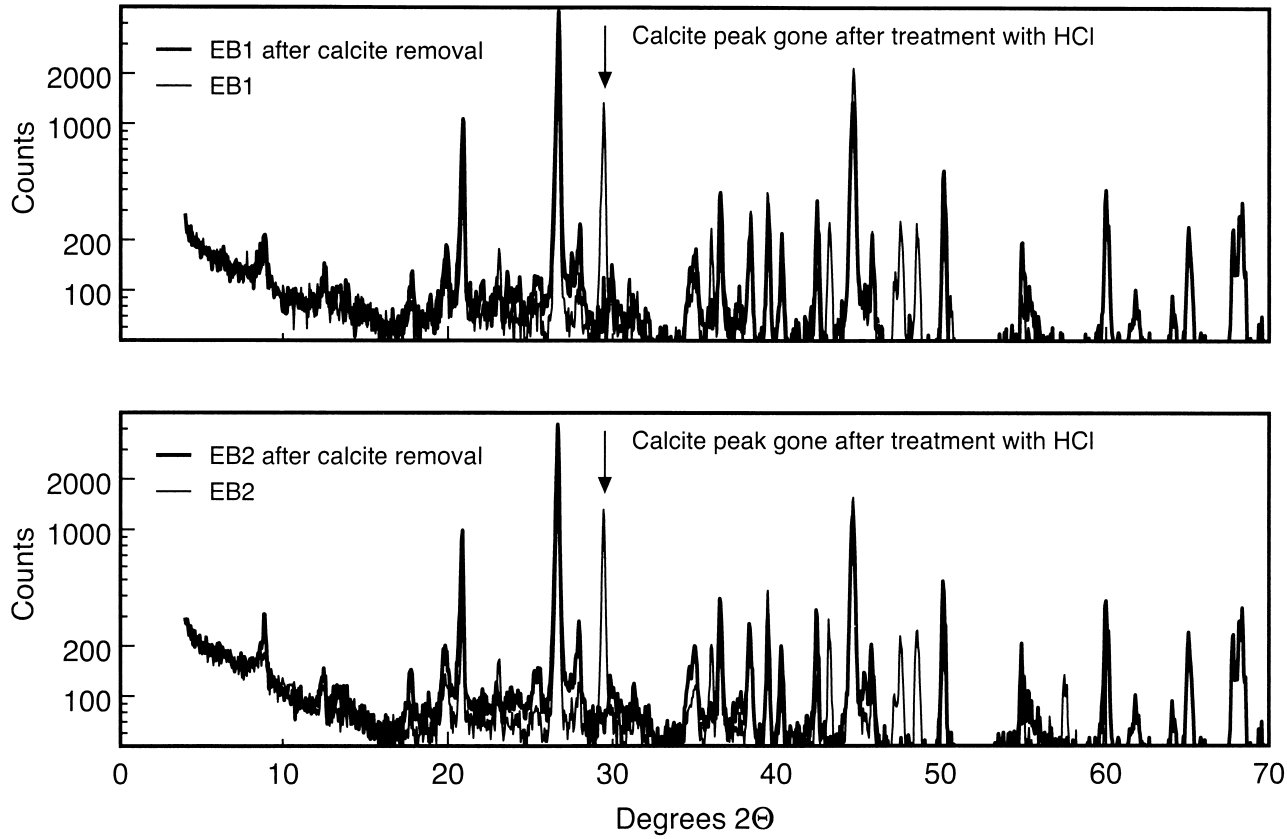

Fig. 2. X-ray diffraction patterns for the Ebro Basin soils EB1 and EB2 before and after the removal of calcite. Observe the disappearance of the calcite peak after treatment.

Reproduced from Soil Science Society of America Journal. Published by Soil Science Society of America. All copyrights reserved.

Table 3. Physical and chemical properties of Iceland Spar and microcrystalline calcite ($CaCO_3$).

Mineral	Surface area	Particle density	Particle size
	$m^2\ g^{-1}$	$g\ cm^{-3}$	μm
Microcrystalline calcite	22	2.66	0.1
Iceland Spar	1.0	2.71	991–1168

to the syringe with the suspension via a tygon tube. A small tension was applied using this syringe to draw out any remaining air. As bubbles formed, the syringe with the suspension was gently tapped to remove these bubbles. This suspension was then injected into the coaxial TDR probe; the suspension had the same solid fraction as the sample measured with air as the background. If the sample was slightly short of reaching the top of the coaxial probe a little more background fluid was added until flush with the top of the probe. Measurements were again made with the TDR and after this the coaxial probe was dismantled and cleaned thoroughly. This procedure was then performed several more times with different background dielectric fluids. Statistical analysis was performed on the grouped data set to determine the 95% confidence interval for each estimate of permittivity. The methodology for this is described in the appendix.

RESULTS

Dielectric Permittivity of Calcite Minerals

The measured permittivity values for Iceland Spar and microcrystalline calcite in the different fluids are presented in Fig. 5. We used an empirical model of the form $\alpha\varepsilon_e^{\beta}$ (where α and β are constants) to interpolate between the measured values to determine the permittivity for the Iceland Spar calcite ($\varepsilon_s = 9.1$), and for the microcrystalline calcite powder ($\varepsilon_s = 8.3$). Figure 5 shows also the uncertainty around the fitted model with the 95% confidence interval. The appendix presents detailed information about the quantification of the uncertainty. The error bars on the microcrystalline calcite show a large uncertainty, however, one of the measurements is located directly underneath the estimate (not seen in Fig. 5) and a fifth measurement was made at a

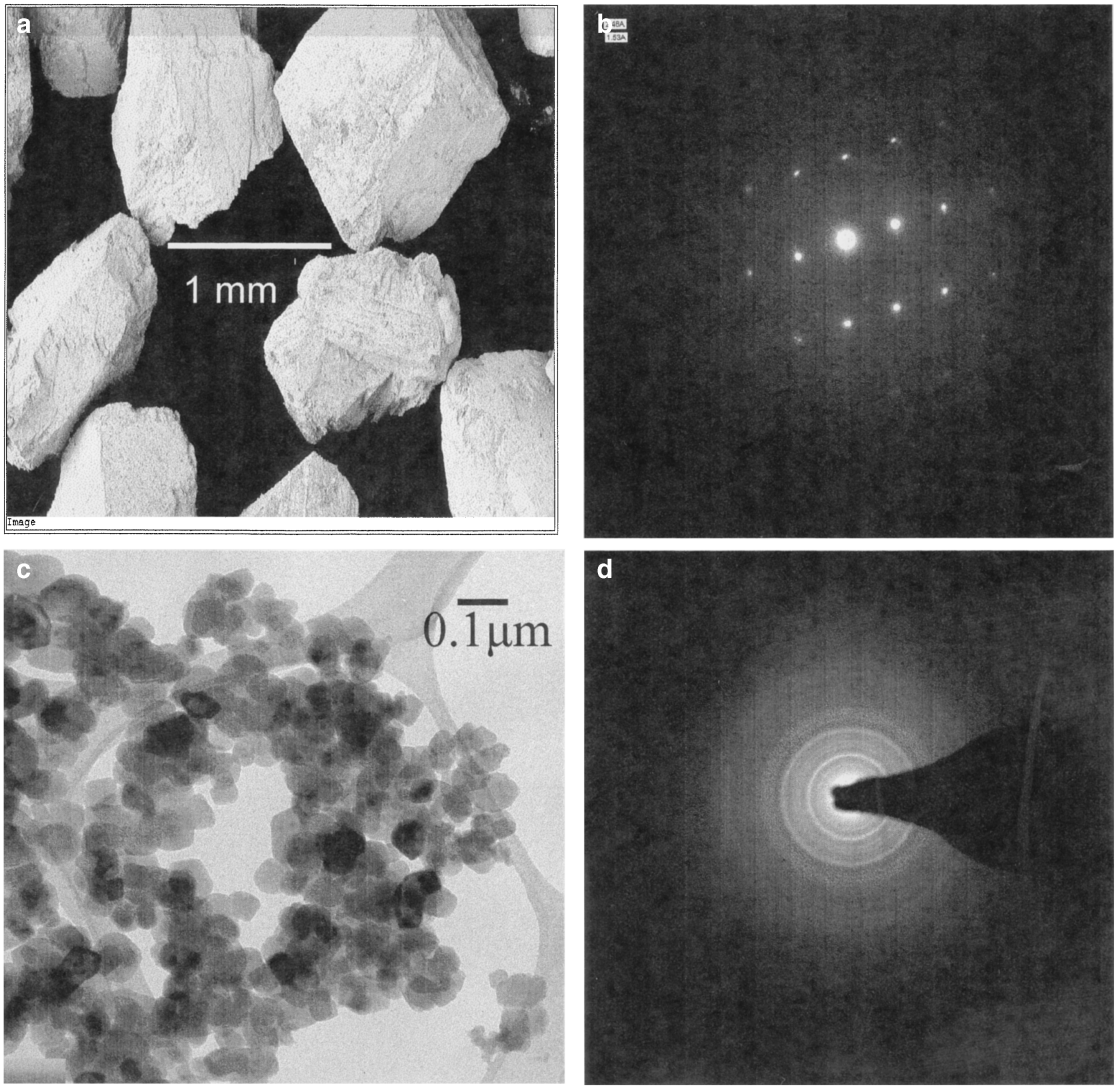

Fig. 3. (a) Scanning electron micrograph of Iceland Spar. (b) Diffraction pattern for Iceland Spar. (c) Transmission micrograph for microcrystalline calcite. (d) Diffraction pattern for microcrystalline calcite.

Reproduced from Soil Science Society of America Journal. Published by Soil Science Society of America. All copyrights reserved.

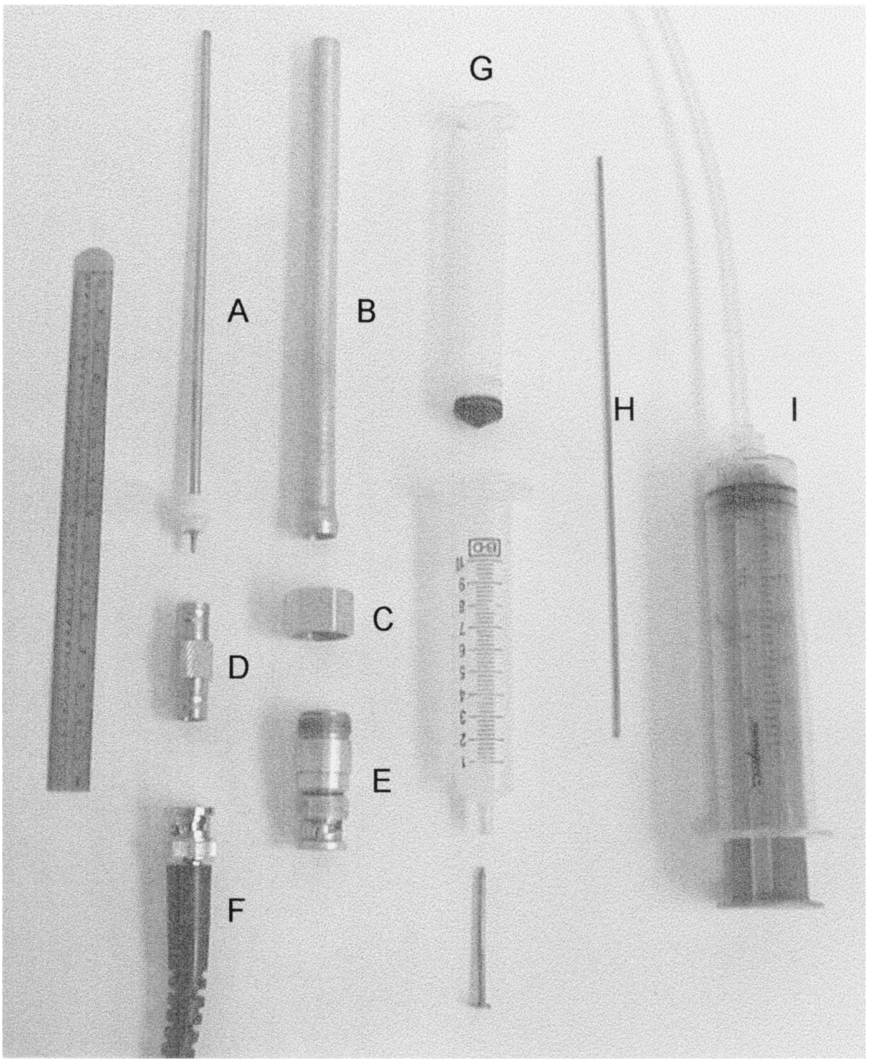

Fig. 4. Photograph of the equipment specifically made for soil dielectric measurements. Internal stainless steel electrode 0.003175 m in diameter and 0.16 m in total length with 0.152 m projecting above the chemical resistant delrin probe head at the base (A); outer brass tube, 0.156 m long with an internal diameter of 0.085 m (B); retaining nut fixing B to E (C); male connector (D); microwave electrical connector (E); coaxial cable (F); syringe assembly for mixing suspension(G); mixing rod (H); syringe used to draw fluid out of the coaxial cell, a similar syringe was used with a piece of tygon tube to connect to G, to apply tension to de-air the suspension (I).

slightly higher permittivity (seen in Fig. 5 underneath the estimate for the Iceland Spar) giving a good correspondence between the measurements and the model. We will also demonstrate that we would expect the solid permittivity value for the micro-crystalline calcite to be lower than for the Iceland Spar as the crystals are less dense. The obtained values are compared with a range of values from the literature in Table 4. The value for Iceland Spar was in good agreement with values obtained from atomistic modeling (Fisler et al., 2000) but was a little higher than values measured using the immersion method for a single calcite crystal (Schmidt, 1902) or values reported in Keller (1989). The values for both the permittivity and particle density quoted from Olhoeft (1981) are in poor agreement with a permittivity value of 8 to 9 and the more generally accepted value of 2.71 g cm^{-3} for the density of crystalline calcite. This may reflect the method of repacking to estimate the permittivity and also the quality of the samples, which were probably natural and may have contained many impurities. The values for the particle density would certainly indicate this. We are confident of our measured Iceland Spar value since the calcite grains were 1 mm in diameter ensuring no air entrapment, which could have biased results. The value for the microcrystalline calcite falls within previously documented permittivity ranges for calcite.

Dielectric Permittivity of Soils

We measured the permittivities of the soil suspensions and used an empirical power function to interpolate between the data points. The obtained curve was then used to calculate the interception of the fitting function with the line $y = x$, this value provides the dielectric permittivity of the soil mineral phase (Robinson and Friedman, 2003). We obtained $\varepsilon_s = 6.0$ for the Ramona soil and $\varepsilon_s = 5.8$ for the Clarence soil, values in close

Reproduced from Soil Science Society of America Journal. Published by Soil Science Society of America. All copyrights reserved.

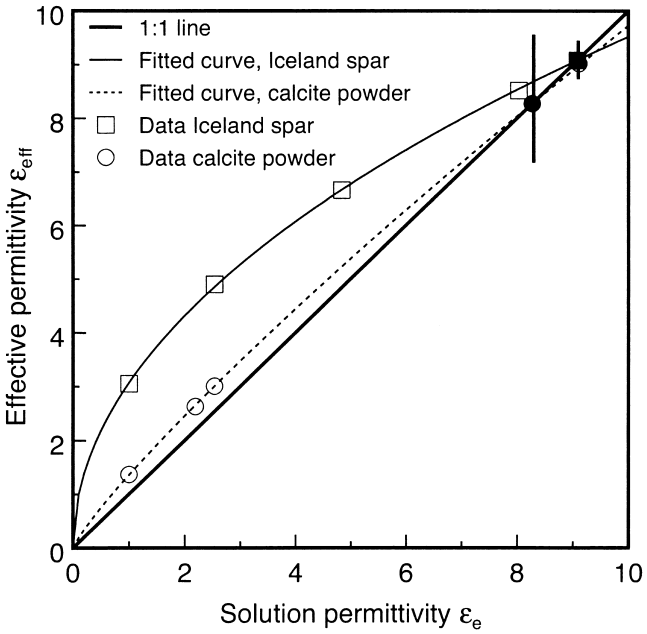

Fig. 5. Effective permittivity of coarse-grained (500 μm) natural calcite sample (Iceland Spar) obtained from a single calcite crystal that was crushed. The calcite powder was a synthetically made sample that was very fine-grained (0.1 μm). The solid symbols represent the estimated permittivity with 95% confidence estimates, Iceland Spar ε_s = 9.1; Micro-crystalline calcite ε_s = 8.3. The forth point for the micro-crystalline calcite lies directly under the estimate, giving perhaps greater confidence in the value of 8.3 than the confidence estimate might suggest.

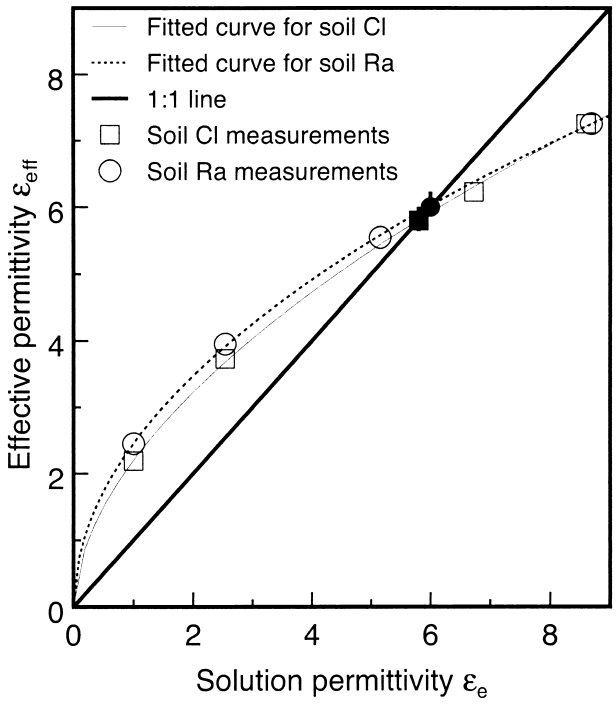

Fig. 6. Effective permittivity of Clarence (Cl) and Ramona (Ra) soils immersed in different dielectric fluids. The solid symbols represent the estimated permittivity with 95% confidence estimates, Cl ε_s = 5.8; Ra ε_s = 6.0.

agreement with their mineralogy (Fig. 6) and values previously measured for illite (Robinson, 2004a).

Figures 7a and 7b present the results for the two Ebro Basin soils. The graphs show the permittivity measured for the unaltered soil mineralogy (ε_s = 6.6 for EB1, ε_s = 6.3 for EB2) and for the soil after treatment to remove the calcite. The permittivity of the soil mineral phase after the removal of the calcite was ε_s = 5.7 for EB1 and 5.8 for EB2, in good agreement with their micaceous mineralogy. However, the permittivity of the soil mineral phase with calcite was not as high as we would expect considering that they have 35 and 41% calcite.

In Table 5 we present results where we predicted the permittivity that we would expect for the whole soil using a simple arithmetic averaging, $\varepsilon_s = \varepsilon_1 f_1 + \varepsilon_2 f_2$ where ε_s is the permittivity of the whole soil, f_1 is the fraction of solid with permittivity ε_1 (micaceous clay), and f_2 is the volume fraction of solid with a permittivity ε_2 (calcite). This assumed that the calcite in the soil had (i) the permittivity of the Iceland Spar, and (ii) the permittivity of the microcrystalline calcite. Finally, for (iii) we calculated the permittivity that the soil calcite must have had to give the permittivity value measured for the whole soil. These calculated values for the pedogenic calcite were both less than 8 and much lower than expected.

DISCUSSION

Differences Between Calcite Permittivity Values

In the introduction (Eq. [1]–[3]) we proposed that the permittivity plays a role in determining the solubility of a crystal in a background fluid. As the permittivity contrast between the crystal and in our case water becomes greater so the change in free energy becomes more negative, and so the crystal is likely to become more soluble. Particle size has been shown to play an important role in the solubility of calcite. Chave and Schmalz (1966) demonstrated that as size decreased so the apparent surface energy increased. Their work indicated that calcite particles under 0.1 μm would be unstable in aqueous systems, tending to be more soluble. They suggested that as particles became smaller the edges

Table 4. Measured and modeled values for the permittivity of calcite obtained from the literature.

	Method of determination	ε_{11}	ε_{33}	ε-average	Density
					g cm^{-3}
Iceland Spar	TDR–immersion			9.1	2.71
Micro-crystalline calcite	TDR–immersion			8.4	2.66
Fisler et al. (2000)	model prediction	9.28	8.3		
Schmidt (1902)	immersion	8.5	8.0		
Keller (1989)				7.8–8.5	
Olhoeft (1981)	repacked granular sample			6.35 (1MHz)	2.931
	repacked granular sample			8.8 (1MHz)	2.555

Reproduced from Soil Science Society of America Journal. Published by Soil Science Society of America. All copyrights reserved.

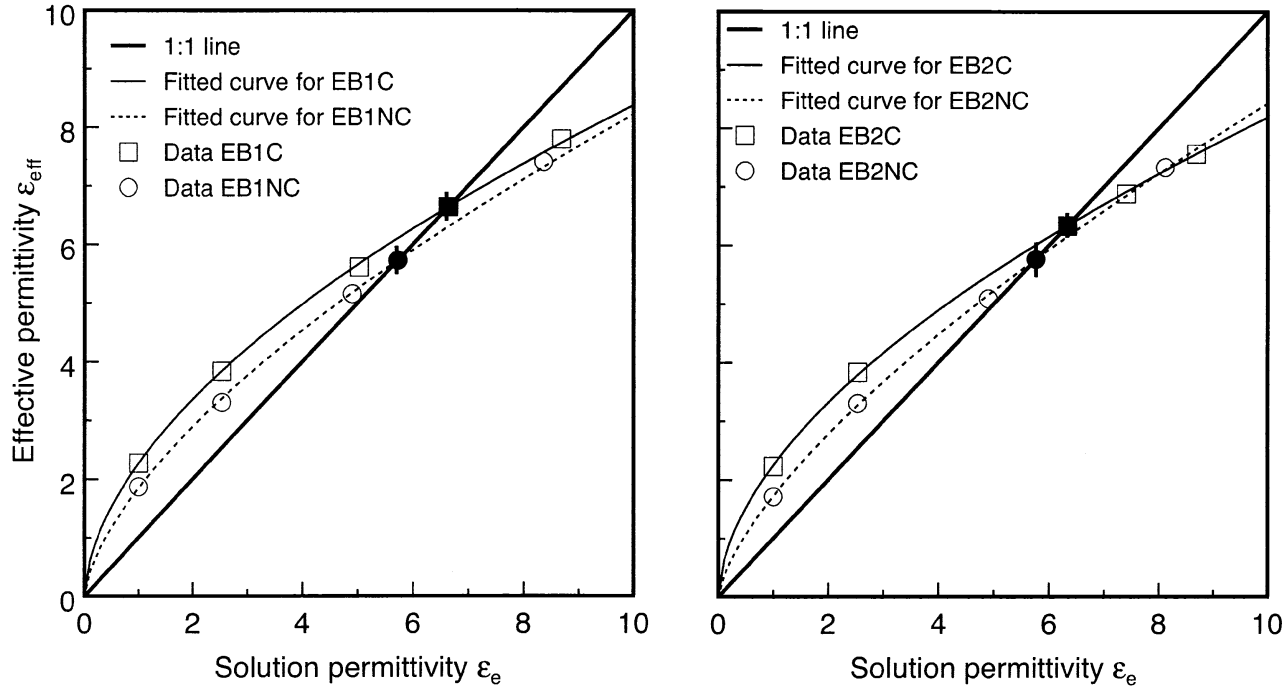

Fig. 7. Effective permittivity of the Ebro Basin soils before (EB1C and EB2C) and after (EB1NC and EB2NC) treatment with acid to remove the calcite. The solid symbols represent the estimated permittivity with 95% confidence estimates, EB1C ε_s = 6.6; EB2C ε_s = 6.3; EB1NC ε_s = 5.7; EB2NC ε_s = 5.8.

and corners play a greater role in the surface energy. They also considered that grinding of calcite could cause a phase transition. It has been shown that calcite can be inverted to aragonite by grinding with a pestle and mortar (Jamieson and Goldsmith, 1960).

Our samples were carefully chosen to provide two extremes of calcite particle size (approximately 1000 and 0.1 μm) without grinding. However, our measurements indicated that although both samples were calcite, the 0.1-μm particles had a lower density. We use this to provide an explanation as to the difference in measured permittivity for each calcite sample. The confidence interval on the microcrystalline calcite measurements overlapped with the Iceland Spar measurements. However, we believe the measurements accurately reflect the calcite properties, and to explain the differences between the measured values of calcite permittivity we use atomistic modeling. This allows us to understand how changes in the crystal density impact the permittivity. Highly sophisticated atomistic models are being continually updated to predict the physical properties of minerals including the permittivity (Gale and Rohl, 2003). However, a good understanding of the important mechanisms can be gained using a more simplistic, semi-physical modeling approach. Polarization mechanisms in solids can be divided into three major categories, electronic, ionic, and orientational; it is the first two of these that are of interest in calcite. The link between the mineral dielectric polarizability, α_D and the measured real part of the dielectric permittivity of the solid, ε_s is given by the Clausius–Mosotti equation:

$$\alpha_D = \frac{1}{b}\left[\frac{V_m\,(\varepsilon_s - 1)}{\varepsilon_s + 2}\right] \qquad [6]$$

where V_m is the molar volume in cubic angstroms {in many reference texts molar volume is given in cm^3 and can be converted to a molar volume in cubic angstroms by: [mole mass/x-ray density ($g\ cm^{-3}$)]/Avogadro's number] $\times 10^{24}$}, b is defined as $4\pi/3$, and ε_s is the real part of the complex dielectric permittivity of the solid (Shannon, 1993; Robinson, 2004b). This simplistic model makes several assumptions; an isotropic distribution of spherical ions in space and all the calculated values of permittivity are average values, taking no account of crystal orientation. The molar volume V_m (cubic Angstroms) is a function of the crystal density indicating the importance of this in determining the polarizability of the crystal. Molar volumes for many minerals can be found in Weast (1984) for example. Shannon (1993) presented a list of ion polarizability values derived from measurements using single crystals of oxide minerals. No measurements were made for the carbonate ion, however, O_2 dominates the polarizability so we can assume that the calcite crystal polarizability is dominated by the Ca ion

Table 5. Dielectric permittivity of the Ebro Basin soils. Calculations of the soil dielectric permittivity (ε_s) were made based on: $\varepsilon_s = \varepsilon_1 f_1 + \varepsilon_2 f_2$ where ε_s is the permittivity of the whole soil, f_1 is the fraction of solid with permittivity ε_1 (soil without the calcite), and f_2 is the volume fraction of solid with a permittivity ε_2 (calcite).†

Soil sample	Measured-ε_s		Predicted-ε_s		
	S	SM	A	B	C
EB1	6.6	5.7	7.1	6.8	7.9
EB2	6.3	5.8	6.9	6.7	7.4

† S = Whole soil; SM = Soil mineral phase after calcite removed; A = $\varepsilon_{SM} f_{SM} + \varepsilon_{Iceland\ Spar} f_{Iceland\ Spar}$; B = $\varepsilon_{SM} f_{SM} + \varepsilon_{microcrystalline\ calcite} f_{microcrystalline\ calcite}$; C = $[\varepsilon_{sS} - (\varepsilon_{SM} f_{SM})]/f_{\%\ Soil\ Calcite}$.

Reproduced from Soil Science Society of America Journal. Published by Soil Science Society of America. All copyrights reserved.

and three oxygen ions summed using the oxide additivity rule (Shannon, 1993). The values of ion polarizabilities used were, 3.16 cubic angstroms for Ca and 2.01 cubic angstroms for O_2 giving a total polarizability of 9.19 cubic angstroms. These values were used in the Clausius–Mosotti equation to predict mineral permittivity values according to:

$$\varepsilon_s = \frac{(3V_m + 8\pi\alpha_D)}{(3V_m - 4\pi\alpha_D)} \quad [7]$$

The model is sensitive to the crystal density, through V_m. By adjusting the density value from 2.71 (Iceland Spar) to 2.66 g cm^{-3} (microcrystalline calcite) the estimated permittivity using Eq. [7] drops from 8.5 to 8.0. The solid permittivity estimate of 8.5 is exceptionally good considering the simplifications in the modeling approach. The half unit, permittivity difference between the two values, caused by altering the molar volume can account fully for the difference in permittivity observed between the Iceland Spar and microcrystalline calcite sample. Thus we suggest that differences in crystal density can account for the observed differences in the crystal permittivity.

By using two confirmed calcite samples we can rule out phase transition as being the mechanism leading to increased permittivity. We would also suggest that based on the arguments presented in Eq. [1] through [3] that our observations are in keeping with measurements of calcite solubility in natural waters in arid environments. In Eq. [3] we demonstrated the importance of the contrast between the permittivity of the crystal ε_e and the background solution ε_b; the greater the contrast the more energetically favorable the transfer is. Thus calcite with a lower permittivity may be part of the solubility mechanism that makes it more soluble in the natural environment. Suarez (1977) and Suarez and Rhoades (1982) found supersaturation of soil solutions to be common in semiarid environments, explaining this by the simultaneous dissolution of silicate minerals and subsequent precipitation of heterogeneously nucleated calcite. Suarez (1983) also found this to be the case for water from areas of the lower Colorado River. Further work might explore in more detail the role of particle size and mineral permittivity on calcite solubility.

We know that soils are not an ideal environment for crystal growth and although micrographs of pedogenic calcite show the classic rhombohedral structure it is likely that the crystal may contain many internal dislocations and defects and these could also reduce the permittivity of the crystal. Accurate dielectric measurement of minerals might be a way of determining their crystallinity, this may help in our understanding of geochemical processes since precipitation and dissolution processes are affected by the permittivity of both the mineral and liquid phase (Israelachvili, 1992).

Implications for Water Content Determination

Equation [4] can be used to estimate the effective permittivity of a two-phase mixture of water and mineral. We found that calculating the effective permittivity of a saturated soil with a porosity of 0.5, using a value of 5.0 for the mineral permittivity then a value of 6.6, representing the soil with 41% calcite, altered the determined effective permittivity from 35.0 to 36.1. Assuming that this would be the maximum difference between permittivity, and applying a refractive index style mixing formula a difference in determined water content of about 0.01 m^3 m^{-3} results. This indicates that even large quantities of pedogenic calcite (40%) are unlikely to substantially affect the determination of water content using a standard calibration.

CONCLUSIONS

Measurements of the dielectric permittivity of calcite samples and arid zone soils with pedogenic calcite are presented. Iceland Spar calcite had a measured permittivity of 9.1 and a microcrystalline calcite had a measured value of 8.3. We explain this difference using an atomistic model based on the difference between the measured density of the two samples. The presence of pedogenic calcite in soils was found to increase the permittivity from 5.7 and 5.8 without calcite to 6.3 and 6.6 for two soils with 35 and 41% calcite, respectively. Modeling calculations suggested that the permittivity of the pedogenic calcite was between 7.4 and 7.9, lower than either of the pure samples. Imperfections in the pedogenic calcite crystal, distortions due to isomorphic substitutions, lower crystal density and/or solid solutions within the crystal might explain these lower permittivity values. We speculate that the lower permittivity observed might be a mechanism that makes pedogenic calcite more soluble and perhaps in part accounts for observed supersaturation of natural waters with respect to calcite.

We also examine the implications of determining water content from dielectric mixing models assuming a permittivity of 5 for the permittivity of the solid. Our calculations suggest that assuming a solid permittivity of 5 instead of 6.6 for a soil with a porosity of 0.5 would only lead to an overestimate of water content of about 0.01 m^3 m^{-3} at saturation.

APPENDIX

Approximate 95% Confidence Interval Estimates

For this study, we assumed that the following multiparameter nonlinear model could adequately describe the laboratory response data:

$$\varepsilon_{\mathrm{eff}_{ij}} = \alpha_i \varepsilon_{eij}^{\beta_i}(1 + \eta_{ij}) \quad [A1]$$

where ε_{eij} represents the j^{th} solution permittivity measurement in the i^{th} experiment, $\varepsilon_{\mathrm{eff}ij}$ represents the corresponding effective permittivity measurement, α_i and β_i represent the model parameters, and η_{ij} represents the random noise component (i.e., the error), which was assumed to be independent and proportional to the measured response. We then log transformed both sides of [A1] to yield:

Reproduced from Soil Science Society of America Journal. Published by Soil Science Society of America. All copyrights reserved.

$$\ln(\varepsilon_{\text{eff}_{ij}}) = \beta_{0i} + \beta_{1i}\ln(\varepsilon_{eij}) + \varsigma_{ij} \quad [A2]$$

which is identical to a standard analysis of covariance (ANOCOVA) model. (A residual assessment performed on this model indicated that the transformed errors satisfied the usual normality assumptions). We then solved [A2] for $\varepsilon_e = \varepsilon_{\text{eff}}$ to produce the crossover point for each experiment; that is,

$$\ln(\varepsilon_{e\,p,i}) = \frac{\beta_{0i}}{1 - \hat{\beta}_{1i}} \quad [A3]$$

An approximate 95% confidence interval for each crossover point was then constructed using a first-order Delta Method calculation (Casella and Berger, 1990). Specifically, the approximate variance of each crossover point estimate was calculated as

$$Var(\varepsilon_{e\,p,i}) = \left(\frac{1}{1 - \hat{\beta}_{1i}}\right) Var(\hat{\beta}_{0i}) + \left[\frac{\hat{\beta}_0}{(1 - \hat{\beta}_{1i})^2}\right]^2 Var(\hat{\beta}_{1i}) + \left[\frac{2\hat{\beta}_0}{(1 - \hat{\beta}_{1i})^3}\right] Cov(\hat{\beta}_{0i}, \hat{\beta}_{1i}) \quad [A4]$$

and ±2 times the square root of this variance estimate was used to create the log confidence intervals. Note that the β parameter variance and covariance estimates used in [A4] were derived from [A2]; that is, the fitted ANOCOVA model. Back-transformed point and interval estimates were then calculated from the variance estimates produced by [A4].

ACKNOWLEDGMENTS

The authors acknowledge funding provided in part by a USDA NRI grant 2002-35107-12507.

REFERENCES

Carmichael, R.S. 1982. Handbook of physical properties of rocks. CRC Press Inc., Boca Raton, FL.

Casella, G., and R.L. Berger. 1990. Statistical inference. Wadsworth and Brooks/Cole, Pacific Grove, CA.

Chave, K.E., and R.F. Schmalz. 1966. Carbonate-seawater interactions. Geochim. Cosmochim. Acta 30:1037–1048.

Cygan, R.T., K. Wright, D.K. Fisler, J.D. Gale, and B. Slater. 2002. Atomistic models of carbonate minerals: Bulk and surface structures, defects, and diffusion. Mol. Simul. 28:475–495.

Davis, J.L., and A.P. Annan. 2002.Ground penetrating radar to measure soil water content. p. 446–463. *In* J.H. Dane and G.C. Topp (ed.) Methods of soil analysis. Part 4. SSSA Book Ser. No. 5. SSSA, Madison, WI.

Fernando, M.J., R.G. Burau, and K. Arulanandan. 1977. A new approach to determination of cation exchange capacity. Soil Sci. Soc. Am. J. 41:818–820.

Fisler, D.K., J.D. Gale, and R.T. Cygan. 2000. A shell model for the simulation of rhombohedral carbonate minerals and their point defects. Am. Mineral. 85:217–224.

Flint, A.L., and L.E. Flint. 2002. Particle density. p. 229–240. *In* J.H. Dane and G.C. Topp (ed.) Methods of soil analysis. Part 4. SSSA Book Ser. No. 5. SSSA, Madison, WI.

Friedman, S.P. 1998. A saturation degree-dependent composite spheres model for describing the effective dielectric constant of unsaturated porous media. Water Resour. Res. 34:2949–2961.

Gale, J.D., and A.L. Rohl. 2003. The general utility lattice program (GULP). Mol. Simul. 29: 291–341.

Heimovaara, T.J. 1993. Design of triple wire time domain reflectometry probes in practice and theory. Soil Sci. Soc. Am. J. 57:1410–1417.

Heimovaara, T.J., and E. de Water. 1993. A computer controlled TDR system for measuring water content and bulk electrical conductivity of soils. Report 41 Laboratory of Physical Geography and Soil Science, University of Amsterdam, Nieuwe Prinsengracht 130 1018 VZ Amsterdam.

Huisman, J.A., C. Sperl, W. Bouten, and J.M. Verstraten. 2001. Soil water content measurements at different scales: Accuracy of time domain reflectometry and ground-penetrating radar. J. Hydrol. (Amsterdam) 245:48–58.

Israelachvili, J. 1992. Intermolecular and surface forces. 2nd ed. Academic Press. New York.

Jackson, M.L., C.M. Lim, and L.W. Zelazny. 1986. Oxides, hydroxides and aluminosilicates. p. 101–150. *In* A. Klute (ed.) Methods of soil analysis. Part 1. 2nd ed. Agron. Monogr. No. 9. ASA and SSSA., Madison, WI.

Jamieson, J.C., and J.R. Goldsmith. 1960. Some reactions produced in carbonates by grinding. Am. Miner. 45:818–827.

Keller, G.V. 1989. Section V electrical properties. *In* R.S. Carmichael (ed) CRC practical handbook of physical properties of rocks and minerals. CRC Press Inc., Boca Raton, FL.

Kunze, G.W., and J.B. Dixon. 1986. Pretreatment for mineralogical analysis. p. 71–100. *In* A. Klute (ed.) Methods of soil analysis. Part 1. 2nd ed. Agron. Monogr. 9. ASA and SSSA, Madison, WI.

Lebron, I., and D.L. Suarez. 1996. Calcite nucleation and precipitation kinetics as affected by dissolved organic matter at 25°C and pH > 7.5. Geochim. Cosmochim. Acta 60:2767–2776.

Lebron, I., and D.L. Suarez. 1998. Kinetics and mechanisms of precipitation of calcite as affected by PCO_2 and organic ligands at 25°C. Geochim. Cosmochim. Acta 63:405–416.

Lebron, I., and D.L. Suarez. 1999. Mechanisms and precipitation rate of rhodochrosite at 25°C as affected by PCO_2 and organic ligands. Soil Sci. Soc. Am. J. 63:561–568.

Lide, D. 1999. Handbook of physics and chemistry. CRC Press, Boca Raton, FL.

Lord Rayleigh. 1892. On the influence of obstacles arranged in rectangular order upon the properties of the medium. Philos. Mag. 34: 481–502.

Maxwell-Garnett, J.C. 1904. Colours in metal glasses and in metallic films. Philos. Trans. Royal Soc. of London. Ser. A. 203:385–420.

McNairn, H., T.J. Pultz, and J.B. Boisvert. 2002. Active microwave remote sensing methods. p. 475–488. *In* J.H. Dane and G.C. Topp (ed.) Methods of soil analysis. Part 4. SSSA Book Ser. No. 5. SSSA, Madison, WI.

Miyamoto, T., T. Annaka, and J. Chikushi. 2003. Soil aggregate structure effects on dielectric permittivity of an andisol measured by time domain reflectometry. Vadose Zone J. 2:90–97.

Nelson, S.O., D.P. Lindroth, and R.L. Blake. 1989. Dielectric properties of selected minerals at 1–22 GHz. Geophysics 54:1344–1349.

Nelson, S.O., and T.-S. You. 1990. Relationships between microwave permittivities of solid and pulverised plastics. J. Phys. D: Appl. Phys. 23:346–353.

Nelson, S.O. 1992. Estimation of permittivities of solids from measurements of pulverised or granular materials. p. 231–271. *In* A. Priou (ed.) Dielectric properties of heterogeneous materials PIER 6. Progress in Electromagnetics Research. Elsevier, Amsterdam.

Olhoeft, G.R. 1979. Tables of room temperature electrical properties for selected rocks and minerals with dielectric permittivity statistics. USGS open file report 79–993. U.S. Gov. Print. Office, Washington, DC.

Olhoeft, G.R. 1981. Electrical properties of rocks. p. 298–329. *In* Y.S. Touloukian and C.Y. Ho (ed.) Physical properties of rocks and minerals. McGraw-Hill/CINDAS Data Series on material properties Volume II-2. McGraw-Hill Book Co., New York.

Paquette, J., H. Vali, and A. Mucci. 1995. Morphology of calcite overgrowths precipitated from strong electrolyte solutions: A TEM study of growth mechanisms. Abstracts of papers, 209th National meeting of the American Chemical Society: Anaheim. American Chemical Society, Washington, DC.

Robinson, D.A., and S.P. Friedman. 2002. The effective permittivity of dense packing of glass beads, quartz sand and their mixtures immersed in different dielectric backgrounds. J. Non Crystalline Solids J. 305:261–267.

Robinson, D.A., and S.P. Friedman. 2003. A method for measuring the solid particle permittivity or electrical conductivity of rocks,

sediments, and granular materials. J. Geophys. Res. B. 108. NO. B2:2076. doi10.1029/2001JB000691.
Robinson, D.A., S.B. Jones, J.M. Wraith, D. Or, and S.P. Friedman. 2003. A review of advances in dielectric and electrical conductivity measurement using time domain reflectometry in soil science. Vadose Zone J. 2:444–475.
Robinson, D.A. 2004a. Measurement of the solid dielectric permittivity of clay minerals and granular samples using a time domain reflectometry immersion method. Vadose Zone J. 2004 3: 705-713.
Robinson, D.A. 2004b. Calculation of the dielectric properties of temperate and tropical soil minerals from ion polarizabilities using the Clausius-Mosotti equation. Soil Sci. Soc. Am. J. 68:1780–1785. (this issue.)
Schmidt, W. 1902. Bestimung der dielecktricitatskonstanten von krystallen mit elektrischen wellen. Ann Physik 9: 919–937.
Shannon, R.D., 1993. Dielectric polarizibilities of ions in oxides and fluorides. J. Appl. Phys. 73:348–366.
Sihvola, A. 1999. Electromagnetic mixing formulas and applications. IEEE Electromagnetic Waves Series No. 47. IEEE, Stevenage, Herts, UK.
Starr, G.C., P. Barak, B. Lowery, and M. Avila-Segura. 2000. Soil particle concentrations and size analysis using a dielectric method. Soil Sci. Soc. Am. J. 64:858–866.
Suarez, D.L. 1977. Ion activity products of calcium carbonate in waters below the root zone. Soil Sci. Soc. Am. J. 41:310–315.
Suarez, D.L. 1983. Calcite supersaturation and precipitation kinetics in the lower Colorado River, All-American canal and East Highline canal. Water Resour. Res. 19:653–661.
Suarez, D.L., and J.D. Rhoades. 1982. The apparent solubility of calcium carbonate in soils. Soil Sci. Soc. Am. J. 46:716–722.
Topp, G.C., J.L. Davis, and A.P. Annan. 1980. Electromagnetic determination of soil water content: Measurements in coaxial transmission lines. Water Resour. Res. 16:574–582.
Topp, G.C., and P.A. Ferre. 2002. Water content. p. 417–446. *In* J.H. Dane and G.C. Topp (ed.) Methods of soil analysis. Part 4. SSSA Book Ser. No. 5. SSSA, Madison, WI.
Weast, R.C. 1984. Handbook of physics and chemistry. CRC Press Inc., Boca Raton, FL.

Reproduced from Soil Science Society of America Journal. Published by Soil Science Society of America. All copyrights reserved.